

Supporting Information

Tuning morphology-dependent localized surface plasmon resonance in quasi-metallic tungsten oxide nanostructures for enhanced photocatalysis

*Yi-Yan Li,^a Chu-Yao Zhong,^a Mei-Xin Li,^a Qiao-Yi Zhang,^a Yibo Chen,^{*a} Zhao-Qing Liu^{*a}, Jin
Zhong Zhang^b*

*^aSchool of Chemistry and Chemical Engineering/Guangzhou Key Laboratory for Clean Energy
and Materials, Guangzhou University, Guangzhou 510006, P. R. China*

*^b Department of Chemistry and Biochemistry, University of California, Santa Cruz, CA 95064,
USA*

CONTENTS

1. Supplementary experimental section	3
1.1 Characterizations.....	3
1.2 Photocatalytic measurement	3
2. Supplementary figures	6
Fig. S1 (a)TEM image, (b) HRTEM images, (c) SAED pattern, and (d, e) EDS mapping of $W_{18}O_{49}$ NW.....	6
Fig. S2 (a)TEM image, (b) HRTEM images, (c) SAED pattern, and (d, e) EDS mapping of $W_{18}O_{49}$ NB.....	6
Fig. S3 SEM images of the $W_{18}O_{49}$ nanostructures obtained with different amount of WCl_6 : (a) 0.0300 g; (b) 0.0500; (c) 0.0700 g; (d) 0.1000 g; (e) 0.1300 g; (f) 0.1500 g; (g) 0.1700 g; (h) 0.2000 g.....	7
Fig. S4 Nitrogen adsorption/desorption isotherms of $W_{18}O_{49}$ samples.....	7
Fig. S5 XPS survey spectra of different $W_{18}O_{49}$ nanostructures.....	8
Fig. S6 The photos of $W_{18}O_{49}$ (a) NW, (b) NB and (c) US.....	8
Fig. S7 Tauc's plot of three different $W_{18}O_{49}$ nanostructures.....	9
Fig. S8 Simulated crystal structure of (a) original $W_{18}O_{49}$ and (b) $W_{18}O_{49}$ with oxygen vacancies (red ball refers to O; blue ball refers to W).....	9
Fig. S9 Adsorption of Cr (VI) on different $W_{18}O_{49}$ samples under dark condition.....	10
Fig. S10 First-order kinetics curve fitting of Cr (VI) reduction under (a) full-spectrum illumination and (c) visible-NIR light irradiation. Corresponding values of the reaction rate coefficient under (b) full-spectrum irradiation and (d) visible-NIR light irradiation.....	10
Fig. S11 Effect of different pH values towards the photoreduction of Cr (VI) under (a, b) visible-NIR light irradiation and (c, d) full-spectrum irradiation.....	11
Fig. S12 (a, b) Cycling photocatalytic results of $W_{18}O_{49}$ US for photoreduction of Cr (VI) under visible-NIR light irradiation. (c) XRD comparison of the fresh and reused $W_{18}O_{49}$ US. (d) SEM image of the reused $W_{18}O_{49}$ US.....	12
Fig. S13 Photoreduction efficiency of 10.00 mg L^{-1} Cr (VI) solution on $W_{18}O_{49}$ US for the main reactive species trapping experiments under visible-NIR light irradiation.....	12
Fig. S14 PL spectra of $W_{18}O_{49}$ NW, NB, and US.....	13
3. Supplementary table.....	14
Table S1 Photoreduction efficiencies towards Cr (VI) of previously reported photocatalysts.....	14
References.....	15

1. Supplementary experimental section

1.1 Characterizations

The surface morphology and crystal microstructure of the nanoparticles were determined using a scanning electron microscope (SEM, JEOL JSM-7001F) and transmission electron microscopy equipped with EDS (TEM, JEM-2100F). The phase composition of the samples was obtained via X-ray diffraction (XRD, PANalytical PW3040/60) with Cu-K α radiation ($\lambda = 0.15418$ nm). The compositions and valence states of the products were investigated with X-ray photoelectron spectroscopy (XPS, Thermo K-Alpha). Photoluminescence (PL) spectra were measured with a spectrophotometer (Hitachi, FL-7000). The UV-vis absorption spectra were acquired on Hitachi UV-3010 spectrophotometer using BaSO₄ as a reference. The specific surface area of the samples was determined by adsorption data with Brunauer-Emmett-Teller (BET) model. The electronic field simulations were performed with the 3D finite element method (3D-FEM, Comsol Multiphysics 5.5). Electronic structure calculations based on a density-functional theory (DFT) were carried out using the CASTEP module (Cambridge Serial Total Energy Package) implemented in the Materials Studio software package. The electron paramagnetic resonance (EPR) measurements were performed at 100 K on a Bruker A300 EPR spectrometer.

1.2 Photocatalytic measurement

The photocatalytic properties of W₁₈O₄₉ nanomaterials were investigated by photocatalytic reduction of Cr (VI). The concentration of Cr (VI) was determined using the diphenylcarbazide (DPC) method. Since DPC reacts with Cr (VI) to form a purple

complex but does not react with Cr (III), so monitoring the concentration of the DPC-Cr(VI) complex can tell the residual concentration of Cr(VI) in the solution. Specifically, 1.0 mL of the collected suspension was added into 9.0 mL 0.20 M H₂SO₄ solution, then 100 μ L newly formed DPC solution was added. After shaking the solution and waiting for 10 minutes, the maximum absorption of DPC-Cr (VI) at 540 nm was measured by UV-vis spectrophotometer (Thermo Orion AquaMate 8000 UV-vis, US). The concentrations of Cr (VI) at different time intervals were obtained according to Lambert-Beer law:

$$A = \varepsilon bc \quad (1)$$

where A is absorbance; ε is molar absorbance coefficient; c is concentration of the sample and b is the thickness of the absorption layer. In our experiments, ε and b are constant with the same material and the same cell. Subsequently, the degradation kinetics of Cr (VI) could be calculated based on the following equations:¹

$$\text{Degradation efficiency\%} = 1 - (C_t/C_0) \quad (2)$$

$$\ln (C_0/C_t) = kt \quad (3)$$

where C_0 and C_t are the concentrations of W₁₈O₄₉ at different time intervals.

1.3 Radical capture and reusability experiments

To verify the photocatalytic mechanism, radical trapping experiments were carried out using AgNO₃ (0.5 mmol), AO (0.5 mmol), and IPA (0.5 mmol) as the capturers of e⁻, h⁺, and •OH, respectively. The experimental process was the same as the degradation experiment in Section 1.2. The stability and reusability of the catalyst were assessed as follows: after the photocatalytic experiments, the samples were recycled by

centrifugation, and treated with 1.0 M HCl for 10 h, then subsequently washed with deionized water and ethanol for several times. The obtained sample was used for the next cycle of photocatalytic experiments with fresh solution of Cr (VI).

2. Supplementary figures

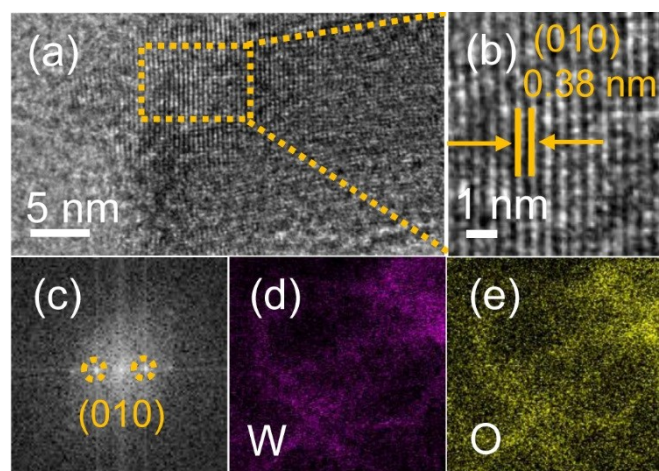


Fig. S1 (a)TEM image, (b) HRTEM images, (c) SAED pattern, and (d, e) EDS mapping of $W_{18}O_{49}$ NW.

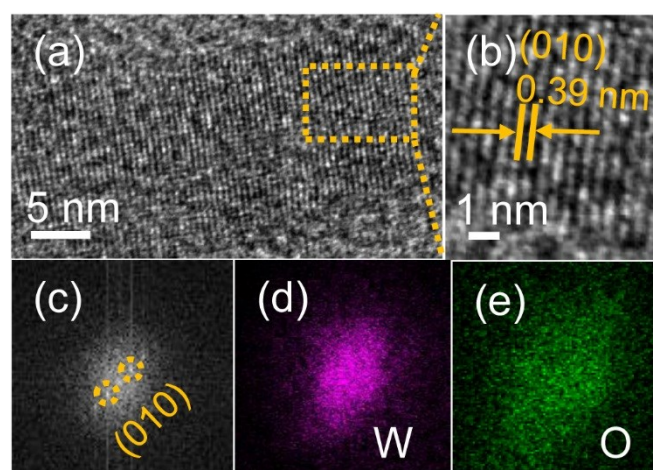


Fig. S2 (a)TEM image, (b) HRTEM images, (c) SAED pattern, and (d, e) EDS mapping of $W_{18}O_{49}$ NB.

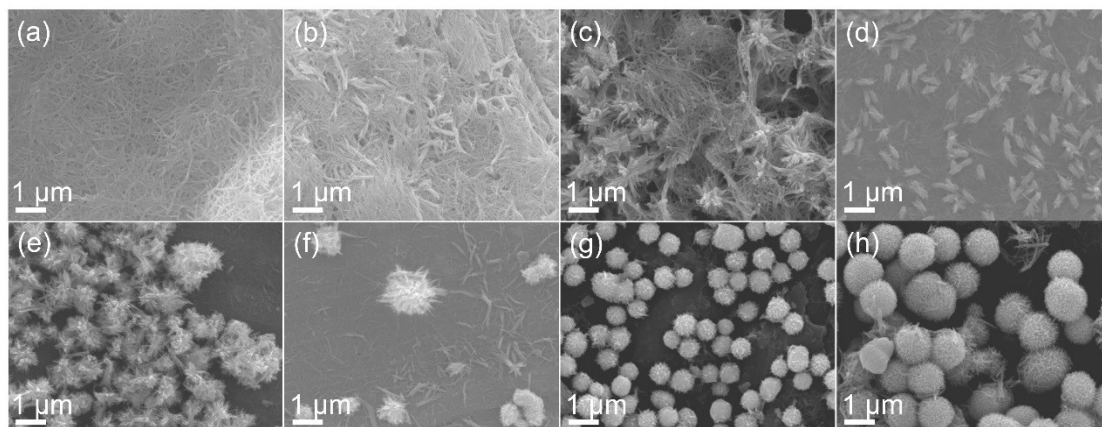


Fig. S3 SEM images of the $W_{18}O_{49}$ nanostructures obtained with different amount of WCl_6 : (a) 0.0300 g; (b) 0.0500; (c) 0.0700 g; (d) 0.1000 g; (e) 0.1300 g; (f) 0.1500 g; (g) 0.1700 g; (h) 0.2000 g.

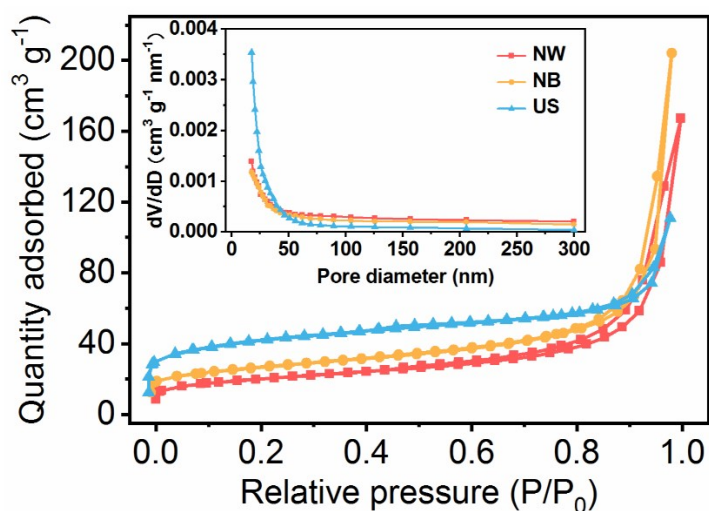


Fig. S4 Nitrogen adsorption/desorption isotherms of $W_{18}O_{49}$ samples.

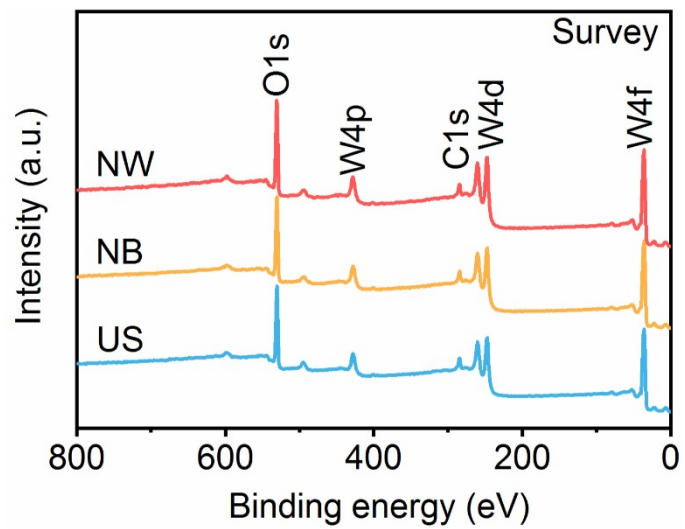


Fig. S5 XPS survey spectra of different $W_{18}O_{49}$ nanostructures.

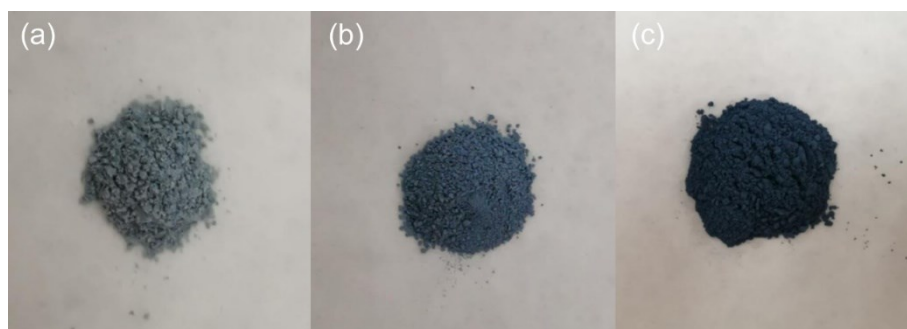


Fig. S6 The photos of $W_{18}O_{49}$ (a) NW, (b) NB and (c) US.

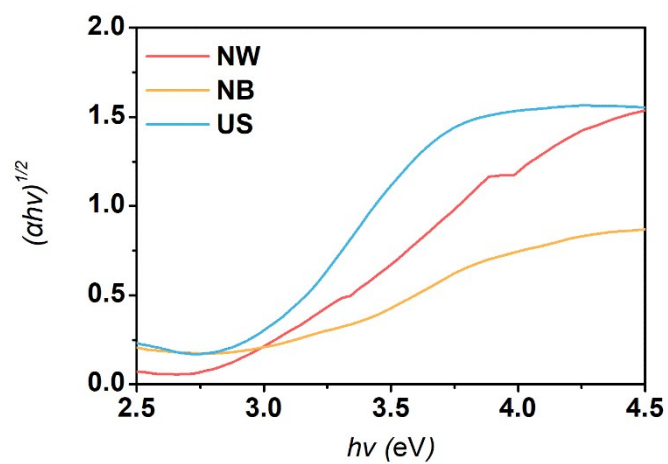


Fig. S7 Tauc's plot of three different $W_{18}O_{49}$ nanostructures.

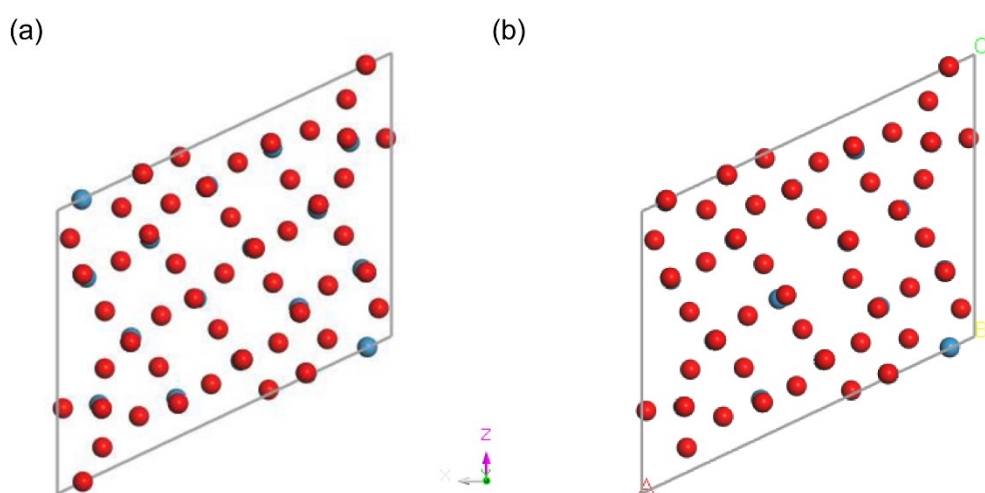


Fig. S8 Simulated crystal structure of (a) original $W_{18}O_{49}$ and (b) $W_{18}O_{49}$ with oxygen vacancies (red ball refers to O; blue ball refers to W).

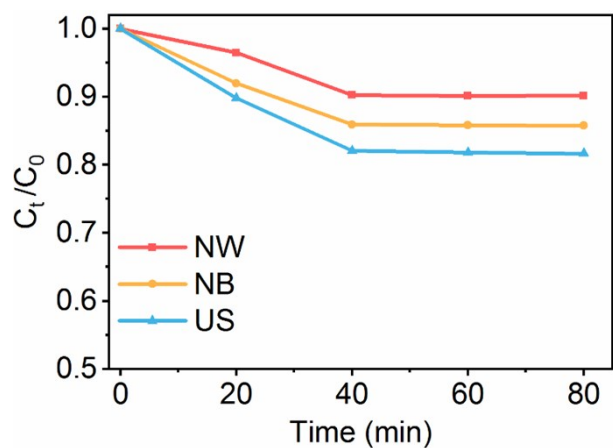


Fig. S9 Adsorption of Cr (VI) on different W₁₈O₄₉ samples under dark condition.

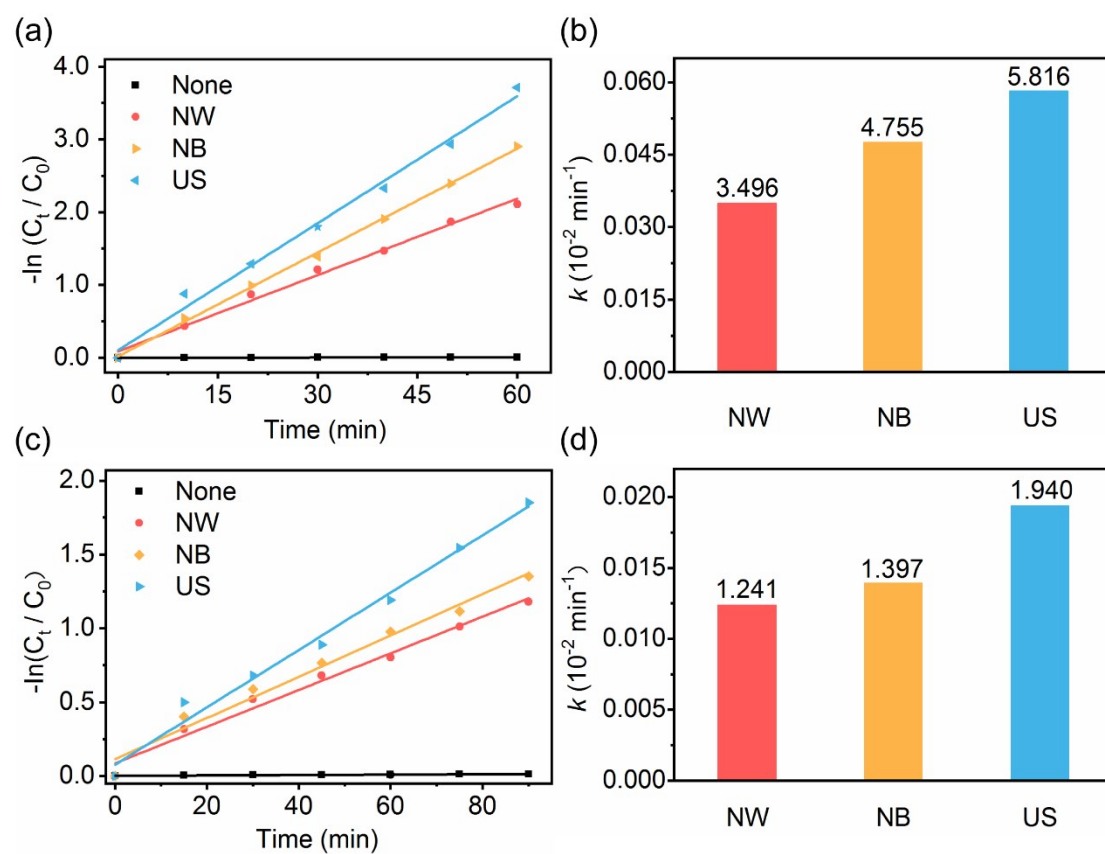


Fig. S10 First-order kinetics curve fitting of Cr (VI) reduction under (a) full-spectrum illumination and (c) visible-NIR light irradiation. Corresponding values of the reaction rate coefficient under (b) full-spectrum irradiation and (d) visible-NIR light irradiation.

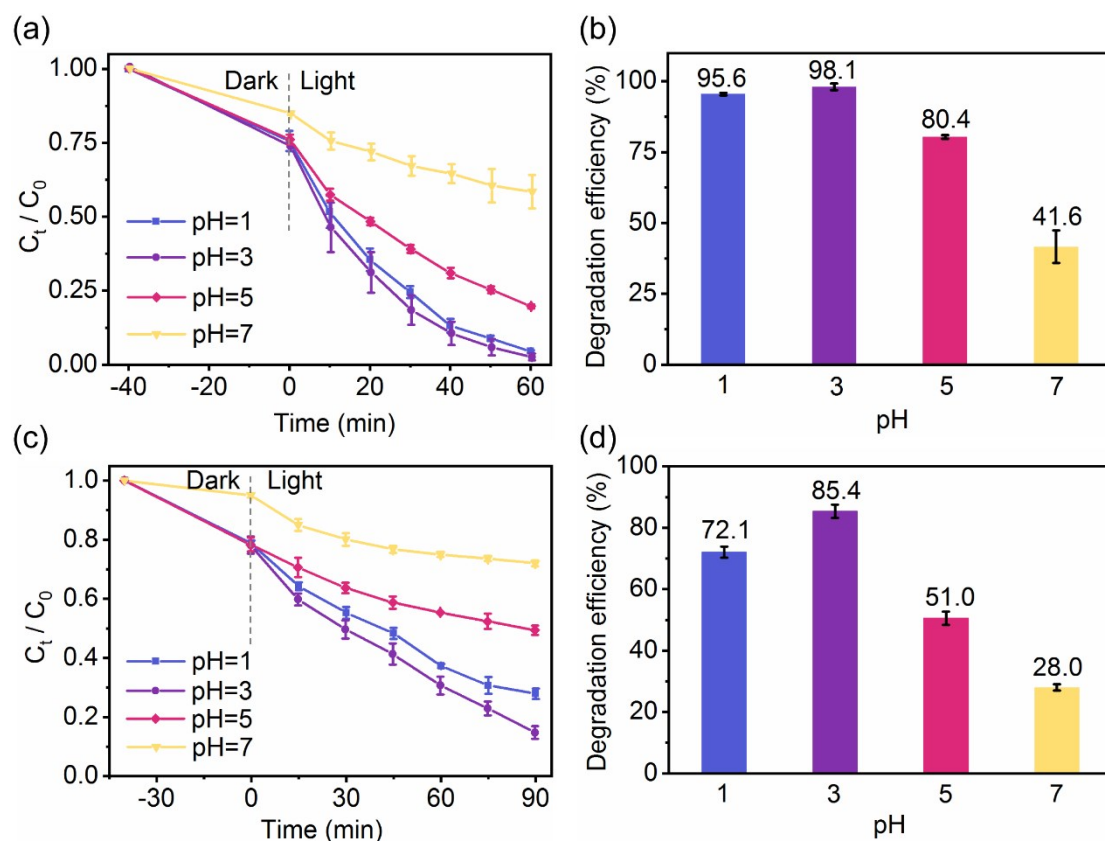


Fig. S11 Effect of different pH values towards the photoreduction of Cr (VI) under (a, b) visible-NIR light irradiation and (c, d) full-spectrum irradiation.

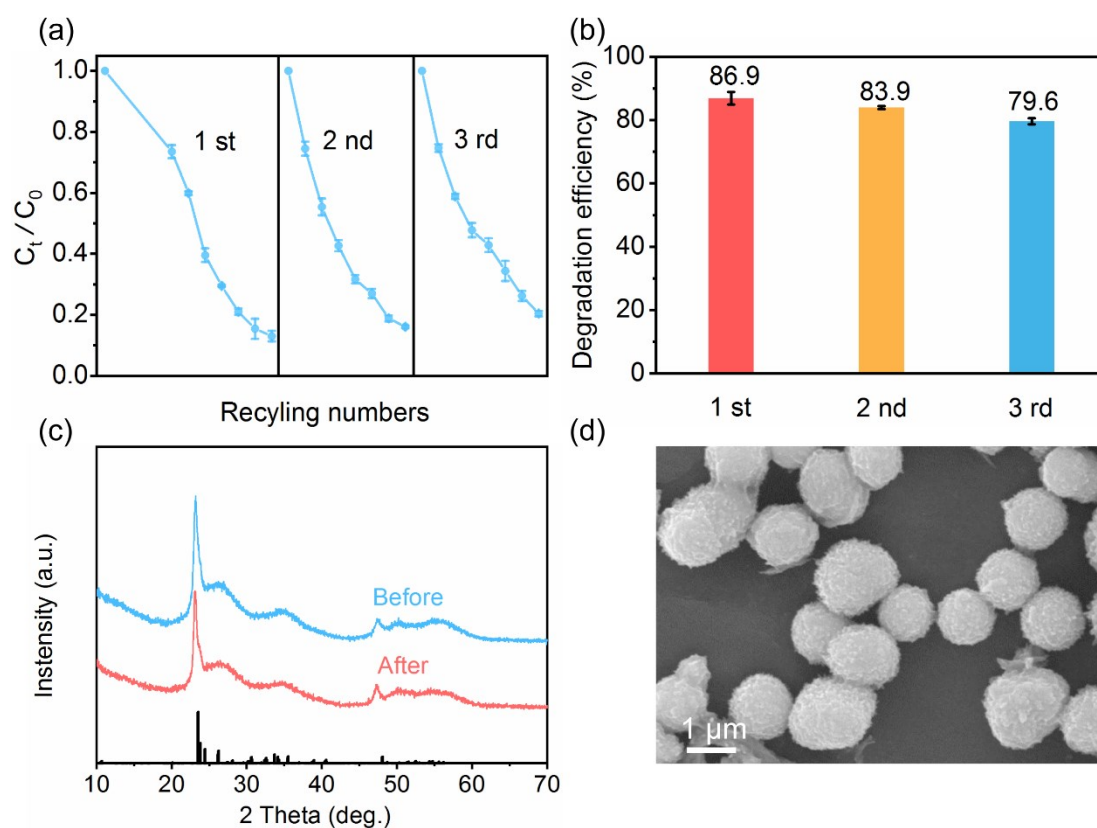


Fig. S12 (a, b) Cycling photocatalytic results of $W_{18}O_{49}$ US for photoreduction of Cr (VI) under visible-NIR light irradiation. (c) XRD comparison of the fresh and reused $W_{18}O_{49}$ US. (d) SEM image of the reused $W_{18}O_{49}$ US.

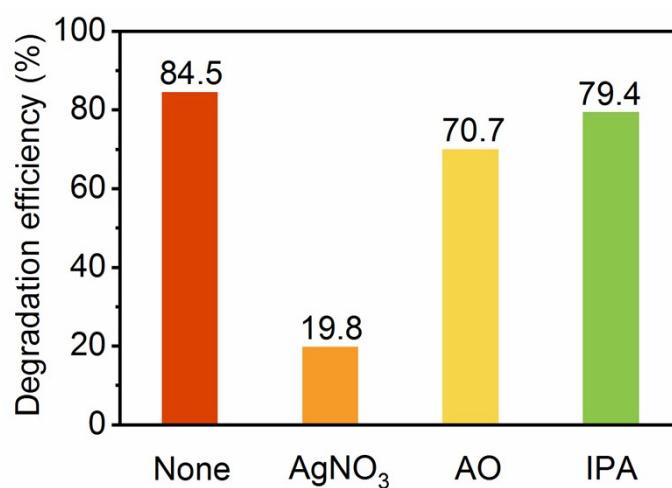


Fig. S13 Photoreduction efficiency of $10.00\ \text{mg L}^{-1}$ Cr (VI) solution on $W_{18}O_{49}$ US for the main reactive species trapping experiments under visible-NIR light irradiation.

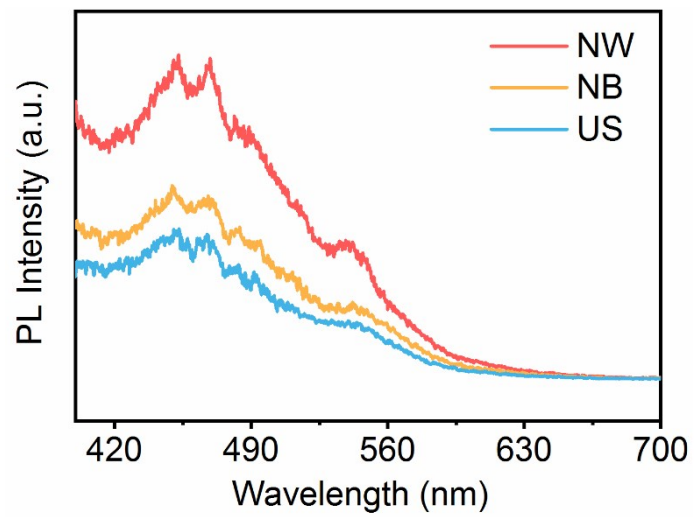


Fig. S14 PL spectra of $W_{18}O_{49}$ NW, NB, and US.

3. Supplementary table

Table S1 Photoreduction efficiencies towards Cr (VI) of previously reported photocatalysts.

Catalysts	Mass of catalysts (mg)	Cr (VI) (mg/L)	pH	<i>t</i> (min)	Degradation efficiency (%)	Ref.
carbon dots-TiO ₂	50.00	10.00	3	120	95	2
CDs-N-TiO ₂	50.00	10.00	5.36	60	94	3
AgIn ₅ S ₈ /Bi ₂ WO ₆	30.00	10.00	-	120	92	4
AgI/BiVO ₄	20.00	15.00	-	100	72	5
Ag ₂ CO ₃ /BiVO ₄	20.00	15.00	-	150	74	6
Ag ₃ VO ₄ /BiVO ₄	20.00	15.00	5.15	150	74.9	7
CoO	15.00	50.00	2	240	56	8
TiO ₂ hollow sphere	30.00	5.00	2.82	120	96	9
Ag/Bi ₂ O ₃ /CuBi ₂ O ₄	40.0	10.0	2	30	96.9	10
Ag/Ag ₃ O ₄	20.0	10.0	5	30	99.0	11
Ag/p-Ag ₂ O/n-BiVO ₄	20.0	15.0	-	100	69.8	12
Urchin-like W ₁₈ O ₄₉	50.00	10.00	3	90	84	This work

References

1. S. He, K. Xiao, X. Chen, Z. Li, T. Ouyang, Z. Wang, M. Guo, Z. Liu, *J. Colloid Interface Sci.*, 2019, **557**, 644.
2. Y. Li, Z. Liu, Y. Wu, J. Chen, J. Zhao, F. Jin, P. Na, *Appl. Catal. B: Environ.*, 2018, **224**, 508.
3. L. Xu, X. Bai, L. Guo, S. Yang, P. Jin, L. Yang, *Chem. Eng. J.*, 2019, **357**, 473.
4. Q. Zhang, M. Wang, M. Ao, Y. Luo, A. Zhang, L. Zhao, L. Yan, F. Deng, X. Luo, *J. Alloys Compd.*, 2019, **805**, 41.
5. W. Zhao, J. Li, B. Dai, Z. Cheng, J. Xu, K. Ma, L. Zhang, N. Sheng, G. Mao, H. Wu, K. Wei, D. Leung, *Chem. Eng. J.*, 2019, **369**, 716.
6. B. Dai, X. Tu, W. Zhao, X. Wang, D. Leung, J. Xu, *Chemosphere*, 2018, **211**, 10.
7. W. Zhao, Y. Feng, H. Huang, P. Zhou, J. Li, L. Zhang, B. Dai, J. Xu, F. Zhu, N. Sheng, D. Leung, *Appl. Catal. B: Environ.*, 2019, **245**, 448.
8. G. Velegraki, J. Miao, C. Drivas, B. Liu, S. Kennou, G. Armatas, *Appl. Catal. B: Environ.*, 2018, **221**, 635.
9. J. Cai, X. Wu, F. Zheng, S. Li, Y. Wu, Y. Lin, L. Lin, B. Liu, Q. Chen, L. Lin, *J. Colloid Interface Sci.*, 2017, **490**, 37.
10. D. Majhi, A. Mishra, K. Das, R. Bariki, B. Mishra, *Chem. Eng. J.* 2020, **31**, 127506.
11. Y. Liu, D. Yang, T. Xu, Y. Shi, L. Song, Z. Yu, *Chem. Eng. J.* 2020, **379**, 122200.
12. W. Zhao, J. Zhang, F. Zhu, F. Mu, L. Zhang, B. Dai, J. Xu, A. Zhu, C. Sun, D. Leung, *Chem. Eng. J.* 2019, **361**, 1352-1362.